Int. J. Solids Structures Vol. 19, No. 6, pp. 553–570, 1983
Printed in Great Britain.

0020-7683/83/060553-18$03.00/0
Pergamon Press Ltd.

BIMODAL OPTIMIZATION OF VIBRATING SHALLOW ARCHES

NIELS OLHOFF and RAYMOND H. PLAUT†
Department of Solid Mechanics, The Technical University of Denmark, Lyngby, Denmark

(*Received* 11 *July* 1982)

Abstract—A bimodal formulation is developed for the problem of maximizing the fundamental vibration frequency of shallow, elastic arches of given span, volume, length, material, and boundary conditions. Arches with different cross-sectional types are considered, and two simultaneous design variables are used, namely the cross-sectional area and arch centerline functions. Results are also presented for arches with circular centerlines.

An effective numerical solution procedure based on successive iterations is constructed, and solutions are obtained for clamped arches of different lengths and minimum constraint values for the cross-sectional area. The numerical results show that bimodality of the fundamental vibration frequency of optimized arches is the rule rather than the exception, and that significant increases of the frequency can be achieved.

1. INTRODUCTION

The vibration properties of a structure determine how it will react to external excitation. In order to avoid resonance conditions, it may be desirable to distribute the amount of structural material in such a way that the fundamental natural frequency of vibration is maximized. This objective is formulated and solved in the present study for shallow elastic arches, using not only variable cross-sectional area but also the arch centerline function as a design variable.

The optimization of structures with respect to vibration frequencies has received much attention[1]. Arches are considered in a few of these studies, but up to now only single functions have been adopted as design variables. Thermann[2] analyzes a simply supported, extensible, circular arch, using the height of solid, fixed-width arch cross-sections as the design variable. He considers the problem of minimizing the total volume of material for given fundamental frequency and includes a constraint of minimum allowable cross-sectional height in the formulation. The design presented for symmetric vibration of an arch with an opening angle of 30° attains this minimum cross-sectional height in the central portion of the span. Smirnov and Troitskii[3] treat a clamped, inextensible, circular arch, in terms of the dual problem of maximizing the fundamental frequency for given total volume. The cross-section is assumed to be circular with varying radius. For an opening angle of 180°, the optimal design takes on the minimum allowable area at three locations, including the center.

In Refs. [4, 5], Blachut and Gajewski use optimal control theory to maximize the fundamental frequency of clamped, circular arches subjected to uniform normal pressure. Free vibration constitutes a special case, associated with zero pressure. The arches are assumed to be inextensible in Ref. [4] and extensible in Ref. [5], and the cross-sections are geometrically similar along the arch, with a prescribed minimum allowable area. Optimization of frequencies for symmetric and antisymmetric modes are first carried out separately. Then a bimodal formulation is presented, in which two frequencies are equal to each other and are maximized together. Resulting designs are shown for arches with opening angles of 90, 120, and 180°. In all these cases, the cross-sectional area has local minima at three locations, including the center.

Finally, shallow (extensible) arches with constant cross-section but variable form are considered by Plaut and Olhoff[6]. The fundamental frequency is maximized for given arch length and volume. It turns out that the optimal form (center line function) is proportional to the fundamental vibration mode of a beam with the same end conditions and subjected to a tensile axial force. If the ends of the arch are clamped, it follows that the optimal form has zero slope at the ends. However, if the prescribed arch length is greater than a certain value, this optimal form is no longer unique, and other forms (e.g. circular) are also optimal.

†Permanent address: Department of Civil Engineering, Virginia Polytechnic Institute and State University, Blacksburg, Virginia, U.S.A.

In the present study, we again consider shallow, elastic arches of given span, length, volume, material, and boundary conditions. But here, the cross-sectional area is allowed to vary along the arch, in addition to the variable form (center line function) of the arch, and the fundamental natural frequency is maximized. In Section 2, the governing equation for vibrations of a shallow arch is presented, and for later comparison purposes lower natural frequencies for the standard case of a uniform circular arch with clamped ends are determined for different values of the arch rise. These results show that the fundamental natural frequency is associated with a symmetric mode for sufficiently low values of the arch rise and an antisymmetric mode otherwise. Simply supported arches exhibit similar behavior.

This strongly indicates that the fundamental frequency of an optimized arch may correspond to two different modes. In order to pursue this conjecture, the problem is formulated as a bimodal optimization problem in Section 3, and as in Ref. [7] the governing equations are derived by the calculus of variations. The mathematical formulation contains single mode optimization as a special case, and will hence provide the correct solution if the fundamental frequency of an optimal arch is actually a simple eigenvalue. As an extension relative to earlier work on optimizing double eigenvalues, two simultaneous design variables are employed in the current paper: the cross-sectional area function and the form of the arch. A minimum constraint value is assumed to be specified for the former design variable, and different cross-sectional geometries are considered. The use of two design variables leads to two simultaneous optimality conditions, which, together with other equations derived in Section 3 for our problem, form the complete set of governing equations. The numerical procedure worked out for solution of this set of nonlinear, strongly coupled integro-differential equations is outlined in the Appendix.

Before solutions to the general formulation with two design variables are obtained for clamped arches, we present in Section 4 a number of results for the special case where the arch form is taken to be circular and only the cross-sectional height is treated as a design variable. These results show that the optimal designs depend significantly on the prescribed values of the arch length parameter and the minimum allowable area. When the length of the clamped arch is equal to its span, the optimal design for beam vibration is obtained, and a comparison to a result reported earlier by Karihaloo and Niordson[8] can be made. As the arch length parameter is increased, the designs change from having minimum area at the center to minimum area at the center and two symmetrically-located positions. Particularly for small minimum constraint values, the maximized fundamental frequency is significantly higher than that of the uniform circular arch with clamped ends.

The general case is treated in Section 5, with varying arch form and cross-sectional height. Even though symmetry is not assumed, the optimal designs are symmetrical. As in Ref. [6], where the area is assumed to be constant and only the form is varied, the optimal forms have zero slope at the clamped ends. For small values of the arch length parameter, the fundamental frequency is increased substantially above that found in Section 4 for the optimal circular arch. However, if the arch length is large enough, the optimal form is no longer unique, and in many cases the circular form is included among the optimal ones. This means that the area distribution determined in Section 4 is then also optimal in terms of the general problem.

Both for circular arches and for the general problem, there is a limit to the maximum attainable fundamental frequency. Associated with any given minimum constraint value for the cross-sectional height, there is a certain value of the arch length parameter, above which the optimal solution does not change. The frequency then cannot be increased by further increases in the arch length. These limiting frequencies are associated with an antisymmetric vibration mode.

The results are summarized in Section 6, and some concluding remarks are given.

2. SHALLOW ARCH VIBRATIONS

We consider the shallow arch depicted in Fig. 1. The arch has length S, span L, form $Y_0(X)$, Young's modulus E, mass density ρ, volume V, cross-sectional area $A(X)$, and moment of inertia $I(X)$. The area and moment of inertia are assumed to be correlated by $I = kA^p$, with the positive factor k and exponent p depending on the cross-sectional geometry. (In the examples

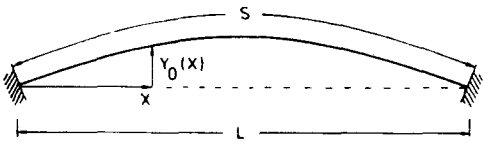

Fig. 1. Shallow arch.

presented in Sections 4 and 5, the cross-section will be rectangular with fixed width w and varying height, which implies $k = 1/(12w^2)$ and $p = 3$.)

The slope of the arch is assumed to be small and the axial force induced by deformation is assumed to be constant along the arch. The arch length S is approximately given by

$$S = L + \frac{1}{2}\int_0^L \left(\frac{dY_0}{dX}\right)^2 dX, \tag{1}$$

and the equation of motion is [9]

$$\frac{\partial^2}{\partial X^2}\left[EI\frac{\partial^2(Y-Y_0)}{\partial X^2}\right] + \frac{E}{2}\frac{\partial^2 Y}{\partial X^2}\left[\int_0^L A^{-1}\,dX\right]^{-1}\int_0^L\left[\left(\frac{dY_0}{dX}\right)^2 - \left(\frac{\partial Y}{\partial X}\right)^2\right]dX + \rho A\frac{\partial^2 Y}{\partial T^2} = 0, \tag{2}$$

where $Y(X, T)$ is the arch configuration at time T. The boundary conditions are

$$Y = 0, \quad \frac{\partial Y}{\partial X} = \frac{dY_0}{dX}, \tag{3a}$$

$$Y = 0, \quad A^p\frac{\partial^2 Y}{\partial X^2} = A^p\frac{d^2Y_0}{dX^2}, \tag{3b}$$

respectively, at a clamped or simply supported end of the arch. For small, harmonic vibrations about $Y_0(X)$, with mode shape $Z(X)$ and angular frequency Ω, i.e.

$$Y(X, T) = Y_0(X) + Z(X)\cos\Omega T, \tag{4}$$

the resulting linear equation in $Z(X)$ becomes

$$(EIZ'')'' - EY_0''\left[\int_0^L A^{-1}\,dX\right]^{-1}\int_0^L Z'Y_0'\,dX - \rho A\Omega^2 Z = 0. \tag{5}$$

It is now convenient to introduce the following nondimensional quantities:

$$x = \frac{X}{L}, \quad y_0 = \frac{Y_0}{2r}, \quad z = \frac{Z}{2r}, \quad \alpha = \frac{AL}{V}, \tag{6}$$

$$\omega^2 = \frac{\Omega^2\rho L^4}{Er^2}, \quad \beta^2 = \frac{(S-L)L}{2r^2} > 0,$$

i.e. coordinate, arch form, vibration mode, cross-sectional area, squared angular vibration frequency, and arch length parameter, respectively. In (6), r is the radius of gyration of the uniform arch having the same length and volume, i.e.

$$r = [k(V/L)^{p-1}]^{1/2}. \tag{7}$$

The dimensionless form of the vibrating arch equation (5) becomes

$$(\alpha^p z'')'' + 4y_0''\left[\int_0^1 \alpha^{-1}\,dx\right]^{-1}\int_0^1 zy_0''\,dx = \omega^2\alpha z, \tag{8}$$

after use of (6) and integration by parts, taking into account boundary conditions in the form of

$$z = 0, \quad z' = 0, \tag{9a}$$

$$z = 0, \quad \alpha^p z'' = 0, \tag{9b}$$

respectively, for clamped or simply supported ends of the arch. Primes now designate differentiation with respect to x.

The design variables in our nondimensional optimization problem are the cross-sectional area $\alpha(x)$ and the arch form $y_0(x)$, and it is our objective to maximize the fundamental natural frequency ω for given span, length, and volume of the arch. A minimum allowable value, $\bar{\alpha}$, will be prescribed for the design variable $\alpha(x)$.

In nondimensional terms the arch span is equal to unity, and the constraint of given total volume is expressed by

$$\int_0^1 \alpha \, dx = 1. \tag{10}$$

The constraint of given arch length, based on (1), is

$$\int_0^1 (y_0')^2 \, dx = \beta^2, \tag{11}$$

where β^2 is termed the arch length parameter. Notice that although shallow arches are considered here, the arch length parameter β^2 *need not be small*, as its definition in (6) involves cross-sectional properties. The minimum constraint to be prescribed for the cross-sectional area $\alpha(x)$ is $\alpha(x) \geq \bar{\alpha}$, where $0 \leq \bar{\alpha} \leq 1$, and can be expressed by means of the real slack variable $g(x)$ as the equality constraint

$$g^2(x) = \alpha(x) - \bar{\alpha}. \tag{12}$$

In mathematical terms, the squared fundamental frequency ω^2 and vibration mode $z(x)$ constitute the eigenvalue and associated eigenfunction of an eigenvalue problem consisting of the differential equation (8) and a set of boundary conditions (9) specified at $x = 0$ and $x = 1$. This problem is easily shown to be self-adjoint, and the Rayleigh quotient for the eigenvalue ω^2 is expressed by

$$\omega^2 = \frac{\int_0^1 \alpha^p (z'')^2 \, dx + 4\left[\int_0^1 \alpha^{-1} \, dx\right]^{-1}\left[\int_0^1 z y_0'' \, dx\right]^2}{\int_0^1 \alpha z^2 \, dx}. \tag{13}$$

It is well known that the Rayleigh quotient is stationary at the mode(s) $z(x)$ among all other kinematically admissible deflection functions.

For comparison purposes later, let us briefly consider the standard case of a clamped, circular arch of uniform cross-section. A circular form is the same as a parabolic one for shallow arches, and we write

$$y_0(x) = 4cx(1 - x), \tag{14}$$

where the nondimensional arch rise c in (14) is related to β by

$$c = \frac{\sqrt{3}}{4}\beta. \tag{15}$$

With $y_0(x)$ given by (14) and $\alpha(x) \equiv 1$, plots of the first four natural frequencies ω as a function of c (which, like β, need not be small for shallow arches) are presented in Fig. 2. The two

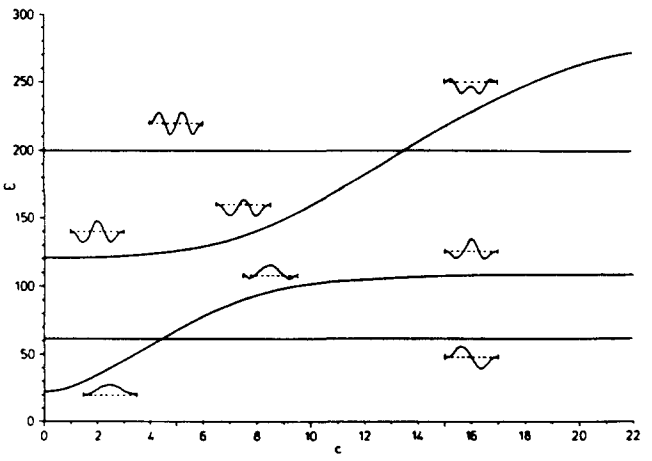

Fig. 2. First four natural frequencies ω vs arch rise c for clamped, circular arches with constant cross-section. Characteristic mode shapes are indicated.

horizontal lines correspond to antisymmetric (inextensible) vibration, which make the second term in (8) equal to zero, and hence ω independent of c. (Thus, they are also valid for a straight, clamped beam.) The other frequencies in Fig. 2 are associated with symmetric vibrations, and their mode shapes change form as c varies. The fundamental frequency corresponds to a symmetric mode if $c \leq 4.464$ and to an antisymmetric mode (with $\omega = 61.673$) if $c \geq 4.464$. In the following, we shall determine the designs that make this frequency a maximum.

3. BIMODAL FORMULATION FOR OPTIMAL DESIGN

A procedure similar to that used in Ref. [7] is employed to derive the governing equations of our optimization problem. We allow for the possibility that the fundamental eigenfrequency ω is double and is associated with *two* vibration modes, $z_1(x)$ and $z_2(x)$. It is convenient to normalize these modes by

$$\int_0^1 \alpha z_i^2 \, dx = 1, \quad i = 1, 2, \tag{16}$$

and to assume that they are mutually orthogonal, i.e.

$$\int_0^1 \alpha z_1 z_2 \, dx = 0. \tag{17}$$

Defining eigenfrequencies ω_1 and ω_2 associated with z_1 and z_2 as

$$\omega_i^2 = \int_0^1 \alpha^p (z_i'')^2 \, dx + 4\left[\int_0^1 \alpha^{-1} \, dx\right]^{-1}\left[\int_0^1 z_i y_0'' \, dx\right]^2, \quad i = 1, 2 \tag{18}$$

in view of (13) and (16), bimodality of ω is expressed by

$$\omega = \omega_i, \quad i = 1, 2. \tag{19}$$

We construct an augmented functional λ by appending to the functional ω_1^2 in (18) the condition $\omega_2^2 = \omega_1^2$ by means of a Lagrangian multiplier γ, and by adjoining conditions (10)–(12), (16) and (17) with the use of Lagrangian multipliers $p\nu$, κ, $p\mu(x)$, $(1-\gamma)\eta_1$, $\gamma\eta_2$, and $\gamma(1-\gamma)\epsilon$. Thus, we write

$$\lambda = (1-\gamma)\left\{\int_0^1 \alpha^p (z_1'')^2 \, dx + 4\left[\int_0^1 \alpha^{-1} \, dx\right]^{-1}\left[\int_0^1 z_1 y_0'' \, dx\right]^2\right\}$$
$$+ \gamma\left\{\int_0^1 \alpha^p (z_2'')^2 \, dx + 4\left[\int_0^1 \alpha^{-1} \, dx\right]^{-1}\left[\int_0^1 z_2 y_0'' \, dx\right]^2\right\}$$

$$-p\nu\left[\int_0^1 \alpha\,dx-1\right]-\kappa\left[\int_0^1 (y_0')^2\,dx-\beta^2\right]$$
$$-\rho\int_0^1 \mu(x)[g^2(x)-\alpha(x)+\tilde{\alpha}]\,dx-(1-\gamma)\eta_1\left[\int_0^1 \alpha z_1^2\,dx-1\right]$$
$$-\gamma\eta_2\left[\int_0^1 \alpha z_2^2\,dx-1\right]-\gamma(1-\gamma)\epsilon\int_0^1 \alpha z_1 z_2\,dx. \tag{20}$$

Note that λ reduces to the appropriate functional for single mode optimal design if $\gamma = 0$ (only z_1 is then involved) or $\gamma = 1$ (only z_2 involved). The mode is then just the fundamental one, and the subscript is superfluous. The interval for γ is

$$0 \le \gamma \le 1, \tag{21}$$

where we have bimodality for $0 < \gamma < 1$. The governing equations of the optimization problem are now obtained as the Euler–Lagrange equations following from the stationarity of λ.

With clamped end conditions

$$z_i(0) = z_i'(0) = z_i(1) = z_i'(1) = 0,\ i = 1, 2 \tag{22}$$

(as well as for other standard end conditions for which the Rayleigh expression (13) is valid), stationarity of λ for arbitrary admissible variations of z_i, $i = 1, 2$, yields

$$(\alpha^p z_i'')'' + 4y_0''\left[\int_0^1 \alpha^{-1}\,dx\right]^{-1}\int_0^1 z_i y_0''\,dx = \eta_i \alpha z_i + \frac{1}{2}\epsilon\alpha e_i(x),\quad i = 1, 2, \tag{23}$$

where $e_1(x) = \gamma z_2(x)$ and $e_2(x) = (1-\gamma)z_1(x)$. Multiplying $(23)_{i=1}$ by z_2 and $(23)_{i=2}$ by z_1, integrating by parts using the boundary conditions, and subtracting the two equations, we obtain the relation $(1-2\gamma)\epsilon = 0$ upon using (16) and (17). With $\gamma \neq 1/2$ in general (the condition may be checked *a posteriori*), we get

$$\epsilon = 0, \tag{24}$$

which implies that inclusion of the orthogonality condition (17) in our formulation does not affect any of the governing equations derived from stationarity of λ in (20). However, (17) implies minor changes in the computational scheme. For example, (17) does not allow z_1 and z_2 to become identical, and γ arbitrary, in cases where the actual solution is single modal, see Ref. [7] where an orthogonality condition was not included in the bimodal formulation.

To determine the Lagrangian multipliers η_i, we multiply (23) by z_i and integrate by parts using the boundary conditions. By means of (16) and (18) we then simply identify η_i as ω_i^2, and may write (23) in the form

$$(\alpha^p z_i'')'' + 4y_0''\left[\int_0^1 \alpha^{-1}\,dx\right]^{-1}\int_0^1 z_i y_0''\,dx = \omega_i^2 \alpha z_i,\quad i = 1, 2. \tag{25}$$

Next, we shall derive the optimality conditions corresponding to our two design variables $y_0(x)$ and $\alpha(x)$. It is well known[10] that multiple eigenvalues are generally not differentiable in the usual sense (Fréchet differentiable) with respect to all possible types of changes in design. This is the case[11] if the design change has a component perpendicular to the intersection "surface" $\omega_1^2 = \omega_2^2$ between the eigenvalue hyper-surfaces $\omega_1^2(y_0, \alpha)$ and $\omega_2^2(y_0, \alpha)$ in the design space y_0, α. However, seeking the maximum ω^2 of a bimodal eigenvalue, it is only necessary to consider the special type of design variations δy_0 and $\delta\alpha$ that confines the varied eigenvalues to the "intersection surface" $\omega_1^2 = \omega_2^2$, and hence involves a move along this "surface". The inclusion of the constraint $\omega_1^2 = \omega_2^2$ for $\gamma \neq 0$ and $\gamma \neq 1$ in our formulation implies a limitation to such variations. Assuming that the "intersection surface" $\omega_1^2 = \omega_2^2$ is sufficiently smooth (Fréchet differentiable) at its maximum, we may subsequently take the variations of the functional λ in the usual fashion.

Now, stationarity of λ with respect to $y_0'(x)$ leads to the first optimality condition,

$$\kappa y_0'(x) = -4\left[\int_0^1 \alpha^{-1}\,dx\right]^{-1}\left[(1-\gamma)z_1'\int_0^1 z_1 y_0''\,dx + \gamma z_2'\int_0^1 z_2 y_0''\,dx\right]. \tag{26}$$

If we multiply (26) by $y_0'(x)$, integrate by parts, make use of (11), solve for κ, use the result in (26), and then differentiate, we get, for $\kappa \neq 0$,

$$y_0''(x) = -\beta^2 \frac{(1-\gamma)z_1''(x)\int_0^1 z_1 y_0''\,dx + \gamma z_2''(x)\int_0^1 z_2 y_0''\,dx}{(1-\gamma)\left[\int_0^1 z_1 y_0''\,dx\right]^2 + \gamma\left[\int_0^1 z_2 y_0''\,dx\right]^2}, \tag{27}$$

which is an implicit equation for the second derivative of the optimal arch form. The determination of $y_0(x)$ is described in the Appendix.

Neither in the derivation of the governing equations nor in the numerical solution procedure for the problem considered in this paper is any assumption made concerning symmetry of the optimal design. However, to discuss possible implications of (27), let us assume for a moment that both arch ends are either clamped or simply supported, the optimal arch form $y_0(x)$ is symmetric, $z_1(x)$ is symmetric, and $z_2(x)$ is antisymmetric. Then

$$\int_0^1 z_2 y_0''\,dx = 0, \tag{28}$$

and hence, from (26), $\kappa = 0$ if $\gamma = 1$, that is, if the fundamental frequency of the optimal symmetric design is single modal with an antisymmetric vibration mode. If this is the case, (27), is invalid, and the optimal arch form $y_0(x)$ is not unique. In contrast to this, $y_0''(x)$ is governed by (27) if $0 \leq \gamma < 1$, which corresponds to cases where the fundamental frequency of the optimal symmetrc design is bimodal or single modal with a symmetric mode. With the use of (28), and the boundary conditions $z_1(0) = z_1(1) = 0$ and $y_0(0) = y_0(1) = 0$, integration of (27) yields

$$y_0(x) = Kz_1(x), \quad K = -\beta^2\left[\int_0^1 z_1 y_0''\,dx\right]^{-1}, \tag{29}$$

i.e. the optimal arch form $y_0(x)$ is simply proportional to the symmetric vibration mode $z_1(x)$ in these latter cases. It is noteworthy that the optimal form $y_0(x)$ of a clamped arch then has zero slope at the ends.

We now return to the general problem. Demanding stationarity of λ with respect to variation of $\alpha(x)$, we obtain the second optimality condition for our problem,

$$\begin{aligned}(1-\gamma)&\left\{p\alpha^{p-1}(z_1'')^2 + 4\alpha^{-2}\left[\int_0^1 \alpha^{-1}\,dx\right]^{-2}\left[\int_0^1 z_1 y_0''\,dx\right]^2 - \omega^2 z_1^2\right\}\\ &+ \gamma\left\{p\alpha^{p-1}(z_2'')^2 + 4\alpha^{-2}\left[\int_0^1 \alpha^{-1}\,dx\right]^{-2}\left[\int_0^1 z_2 y_0''\,dx\right]^2 - \omega^2 z_2^2\right\}\\ &= p[\nu - \mu(x)],\end{aligned} \tag{30}$$

while stationarity with respect to variation of $g(x)$ gives

$$\mu(x)g(x) = 0. \tag{31}$$

We identify by x_u and x_c the sub-intervals in which $g(x) \neq 0$ and $g(x) = 0$, respectively, where x_u and x_c make up the entire interval $0 \leq x \leq 1$. For $x \in x_u$, we have $\mu(x) = 0$ by (31) and $\alpha(x) > \bar{\alpha}$ by (12), i.e. the cross-sectional area is unconstrained. For $x \in x_c$, we have $\alpha(x) = \bar{\alpha}$ from (12), i.e. the cross-sectional area is constrained. Consequently, for the optimal design, $\alpha(x)$ is governed by (30) with $\mu(x) = 0$ for $x \in x_u(\alpha(x) > \bar{\alpha})$, and $\alpha(x)$ is equal to $\bar{\alpha}$ for $x \in x_c$.

In order to construct a convergent iterative solution procedure for our problem, it is useful to introduce the dimensionless bending moment functions

$$m_i(x) = \alpha^p(x) z_i''(x), \quad i = 1, 2, \tag{32}$$

so as to eliminate the second derivatives $z_i''(x)$ and obtain a higher numerical value of the power of $\alpha(x)$ in the optimality condition (30). Doing this, the condition takes the following form in the unconstrained sub-intervals, where we have $\mu(x) = 0$:

$$A(m_i, \gamma) \cdot \alpha^{-(p+1)} + B(\alpha, y_0, z_i, \gamma) \cdot \alpha^{-2} - C(z_i, \gamma, \omega^2, \nu) = 0, \quad x \in x_u, \tag{33}$$

where the coefficient functions A and C, and the constant coefficient B, are defined by

$$A(m_i, \gamma) = (1-\gamma) m_1^2 + \gamma m_2^2, \tag{34a}$$

$$B(\alpha, y_0, z_i, \gamma) = \frac{4}{p}\left[\int_0^1 \alpha^{-1}\,dx\right]^{-2}\left\{(1-\gamma)\left[\int_0^1 z_1 y_0''\,dx\right]^2 + \gamma\left[\int_0^1 z_2 y_0''\,dx\right]^2\right\}, \tag{34b}$$

$$C(z_i, \gamma, \omega^2, \nu) = \nu + \frac{\omega^2}{p}[(1-\gamma) z_1^2 + \gamma z_2^2]. \tag{34c}$$

Due to (21) and the fact that $\nu \geq 0$, these coefficients are non-negative.

Denoting by $\alpha_u(x)$ those segments of the solution $\alpha(x)$ to the nonlinear, algebraic equation (33) for which we have $\alpha(x) > \tilde{\alpha}$, the optimal cross-sectional area function $\alpha(x)$ and the sub-intervals x_u and x_c are defined over the entire interval $0 \leq x \leq 1$ by the formula

$$\alpha(x) = \begin{cases} \alpha_u(x) (\text{if} > \tilde{\alpha}), & x \in x_u \\ \tilde{\alpha}, & x \in x_c. \end{cases} \tag{35}$$

The expressions for $\alpha_u(x)$ in the standard cases of $p = 1, 2$, or 3 are easily determined by solving (33) for $\alpha(x) = \alpha_u(x) > \tilde{\alpha}$, $x \in x_u$:

$$p = 1: \quad \alpha_u(x) = \left[\frac{A+B}{C}\right]^{1/2}; \tag{36a}$$

$$p = 2: \quad \alpha_u(x) = \left[\frac{A+D}{2C}\right]^{1/3} + \left[\frac{A-D}{2C}\right]^{1/3}, \quad D = \left[A^2 - \frac{4B^3}{27C}\right]^{1/2}; \tag{36b}$$

$$p = 3: \quad \alpha_u(x) = \left[\frac{2A}{[B^2 + 4AC]^{1/2} - B}\right]^{1/2}. \tag{36c}$$

In order to determine the coefficients A, B and C defined by (34), we obtain the modes $z_i(x)$ and moments $m_i(x)$ by solution of the differential equation (25) for the vibrating arch with appropriate boundary conditions, and the optimal arch form $y_0(x)$ and its first and second derivatives are found from the optimality condition (27). It will be outlined below how the remaining quantities are determined.

If we substitute (35) into the volume constraint (10), we obtain

$$\int_{x_u} \alpha_u(x)\,dx + \tilde{\alpha} \int_{x_c} dx = 1. \tag{37}$$

Assuming the coefficients A and B to be known, together with the second term in the expression (34c) for C, (37) constitutes an implicit equation for the Lagrangian multiplier ν, if we take (34c) and the appropriate expression for $\alpha_u(x)$ in (36) into account. When ν is determined, the function $\alpha(x)$, and thereby the sub-intervals x_u and x_c, are determined by (34)–(36).

Substituting (35) into (18), we get

$$\omega_i^2 = \int_{x_u} \alpha_u{}^p\,(z_i'')^2\,dx + \bar{\alpha}^p \int_{x_c} (z_i'')^2\,dx + 4\left[\int_{x_u} \alpha_u{}^{-1}\,dx + \bar{\alpha}^{-1}\int_{x_c} dx\right]^{-1}\left[\int_0^1 z_i y_0''\,dx\right]^2,\ i = 1, 2. \tag{38}$$

These equations give us the optimal fundamental eigenvalue ω^2, which is used in (34c) and also in connection with the determination of γ for (34). Thus,

$$\begin{aligned} &\text{if}\quad \omega_1 < \omega_2 : \omega = \omega_1, \quad \gamma = 0; \\ &\text{if}\quad \omega_2 < \omega_1 : \omega = \omega_2, \quad \gamma = 1. \end{aligned} \tag{39}$$

A value of the Lagrangian multiplier γ ensuring a bimodal optimal fundamental frequency $\omega = \omega_1 = \omega_2$ is determined as a solution to the following equation, which is obtained by substituting (38) into the bimodality condition expressed as $\omega_2{}^2 - \omega_1{}^2 = 0$:

$$\int_{x_u} \alpha_u{}^p[(z_2'')^2 - (z_1'')^2]\,dx + \bar{\alpha}^p \int_{x_c} [(z_2'')^2 - (z_1'')^2]\,dx + 4\left[\int_{x_u} \alpha_u{}^{-1}\,dx + \bar{\alpha}^{-1}\int_{x_c} dx\right]^{-1}\left\{\left[\int_0^1 z_2 y_0''\,dx\right]^2 - \left[\int_0^1 z_1 y_0''\,dx\right]^2\right\} = 0. \tag{40}$$

Clearly, (40) provides an implicit equation for γ, when we substitute into it the appropriate expression for $\alpha_u(x)$ from (36), with A, B, and C expressed by (34).

In summary, the general optimization problem is governed by the eqns (16), (17), (21), (25), (27) and (34)–(40), together with appropriate boundary conditions. The value of p, the arch length parameter β^2, and the minimum area $\bar{\alpha}$ are specified. The unknowns to be determined are the optimal eigenvalue ω^2, the optimal cross-sectional area function $\alpha(x)$ (and thereby the sub-intervals x_u and x_c), the optimal arch form $y_0(x)$, the eigenfunctions $z_1(x)$ and $z_2(x)$, and the Lagrangian multipliers ν and γ. The method of solution is outlined in the Appendix.

4. OPTIMIZATION OF CIRCULAR ARCHES WITH CLAMPED ENDS

We present from now on a number of optimal design results for clamped arches with solid cross-sections of variable height and fixed width, i.e. the case $p = 3$ is considered. In this section we only use the cross-sectional area function $\alpha(x)$ as a design variable, and assume that the form of the shallow arch is circular and given by (14). Hence, for the problem considered here, (14) replaces (27) and (11) drops out in the mathematical formulation for optimal design outlined in the previous section. We will call the dimensionless quantity c in (14) the arch rise parameter, in order to distinguish it from the arch length parameter β^2, which is related to c by (15). The optimal area function $\alpha(x)$ is determined for various values of c and the geometric (minimum area) constraint $\bar{\alpha}$. In all cases, we find the optimal design to be symmetrical within double precision computational accuracy.

Representative designs $\alpha(x)$ are illustrated in Figs. 3–7, along with associated fundamental

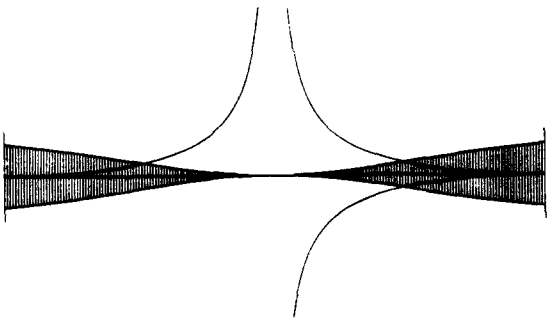

Fig. 3. Geometrically unconstrained optimal design ($\bar{\alpha} = 0$) of a clamped straight beam ($c = 0$, $p = 3$). The optimal dimensionless frequency ω is $\omega = 59.7$ (bimodal), and $\omega/\omega_{cu} = 2.67$.

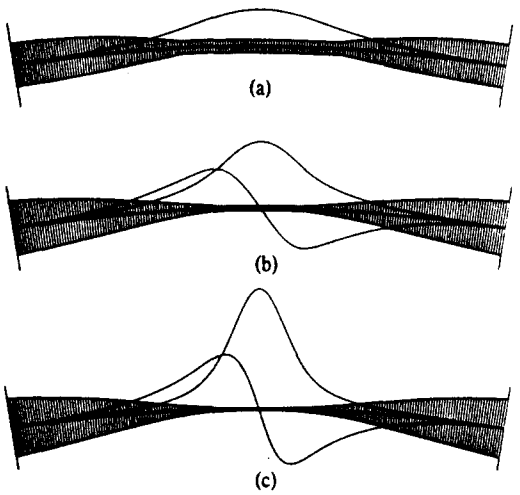

Fig. 4. Optimal designs of clamped circular arches with $c = 3$ (and $p = 3$). (a) Design for $\bar{\alpha} = 0.5$ (active constraint), $\omega = 56.1$ (single modal), $\omega/\omega_{cu} = 1.24$. (b) Design for $\bar{\alpha} = 0.2$ (active constraint), $\omega = 63.4$ (bimodal), $\omega/\omega_{cu} = 1.40$. (c) Optimal design for $0 \le \bar{\alpha} \le 0.084$ (inactive constraint), $\omega = 64.8$ (bimodal), $\omega/\omega_{cu} = 1.43$.

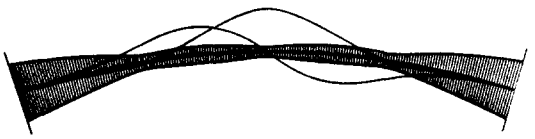

Fig. 5. The optimal design of a clamped circular arch with $c = 6$ (and $p = 3$) for $0 \le \bar{\alpha} \le 0.40$ (inactive constraint). The optimal frequency $\omega = 78.7$ is bimodal, and $\omega/\omega_{cu} = 1.28$.

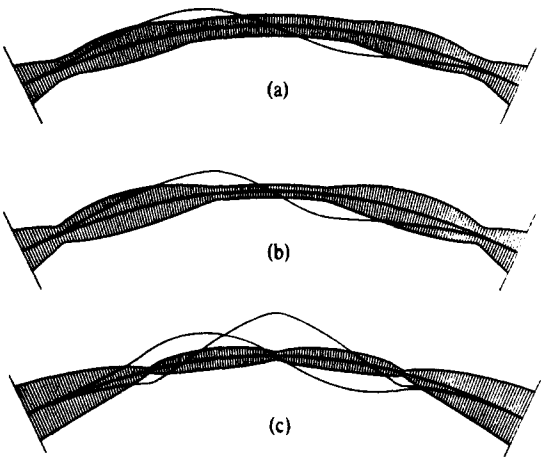

Fig. 6. Optimal designs of clamped circular arches with $c = 9$ (and $p = 3$). (a) Design for $\bar{\alpha} = 0.8$ (active constraint), $\omega = 74.7$ (single modal), $\omega/\omega_{cu} = 1.21$. The area function is, in fact, optimal for all problems with $\bar{\alpha} = 0.8$ and $c \ge 6$. (b) Design for $\bar{\alpha} = 0.5$ (active constraint), $\omega = 81.0$ (single modal), $\omega/\omega_{cu} = 1.31$. The area function is optimal for all problems with $\bar{\alpha} = 0.5$ and $c \ge 8$. (c) Optimal design for $0 \le \bar{\alpha} \le 0.18$ (inactive constraint), $\omega = 82.8$ (bimodal), $\omega/\omega_{cu} = 1.34$.

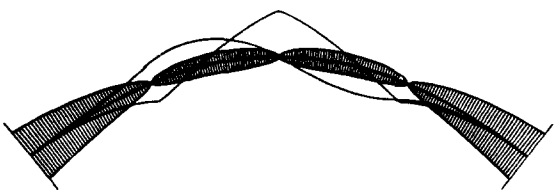

Fig. 7. The optimal design of a clamped circular arch with $c = 15$ (and $p = 3$) for $0 \le \bar{\alpha} \le 0.01$ (inactive constraint). The optimal frequency $\omega = 83.4$ is bimodal, and $\omega/\omega_{cu} = 1.35$.

modes $z_1(x)$ and $z_2(x)$ if the solution is bimodal, and the appropriate single mode otherwise. The optimal fundamental frequencies ω of the optimal designs are stated in the figure captions, together with the ratio ω/ω_{cu} between ω and the fundamental frequency ω_{cu} of a clamped, circular arch that has constant cross-section and has the same length, span, volume, and material as the optimal arch. The dependence of ω_{cu} on c can be seen in Fig. 2.

The special case $c = 0$ corresponds to optimization of a transversely vibrating, clamped, straight beam with varying height of solid, rectangular cross-sections of fixed width. Only in the limiting case of geometrically unconstrained design ($\bar{\alpha} = 0$) is the optimal solution bimodal. This optimal design, which is depicted in Fig. 3, has an inner separation (Type II singularity, see Ref. [12] for the case $p = 2$) at the center, where the cross-sectional area, bending moment, and shear force vanish. Each half of the beam is thus a scaled version of the optimal, vibrating cantilever obtained by Niordson and Karihaloo [8]. (If we square the clamped–clamped beam eigen frequency ω given in the caption of Fig. 3 and transform it to a beam of twice the volume and length by means of the formula given in (6), we obtain perfect agreement with the optimal eigenvalue stated for the cantilever in Ref. [8].)

Results for $c = 3$ and different values of $\bar{\alpha}$ are shown in Fig. 4. For $\bar{\alpha} = 0.5$, the optimal design is single modal and the mode is symmetric, as seen in Fig. 4(a). For $\bar{\alpha} = 0.2$, the optimal design is bimodal (Fig. 4b) and associated with both a symmetric and an antisymmetric fundamental vibration mode. In both these cases, the geometric constraint is active in the central portion of the span. For $\bar{\alpha} < 0.084$, this constraint is inactive and the optimal (bimodal) design is shown in Fig. 4(c). This design constitutes in particular the geometrically unconstrained ($\bar{\alpha} = 0$) optimal design for $c = 3$, which thus has finite minimum area (equal to 0.084) in contrast to the solution for $c = 0$ shown in Fig. 3. (The transition from zero to finite minimum area in the geometrically unconstrained optimal designs is found to take place at a value of c between 1 and 2.)

If the arch rise parameter has the value $c = 6$, the geometric constraint $\alpha(x) \geq \bar{\alpha}$ is not active if $\bar{\alpha} < 0.40$, and the corresponding optimal (bimodal) design is depicted in Fig. 5. The area function of this design, which also constitutes the geometrically unconstrained optimal solution for $c = 6$, is smallest at midspan (equal to 0.40) like the designs in Figs. 3 and 4(c), but the area function now exhibits two other local minima.

Results for $c = 9$ associated with different $\bar{\alpha}$ values are presented in Fig. 6. For $\bar{\alpha} = 0.8$ and 0.5 (Figs. 6a, b), the designs are single modal with an antisymmetric mode. For $\bar{\alpha} < 0.21$ (Fig. 6c), the geometric constraint is inactive and the design is bimodal. The area of this geometrically unconstrained optimal design for $c = 9$ is now smaller ($\alpha = 0.18$) at the two symmetrically placed locations than at mid-span ($\alpha = 0.34$).

Finally, the optimal design for $c = 15$ and $\bar{\alpha} \leq 0.01$ is depicted in Fig. 7. The optimal design is bimodal and has smaller area ($\alpha = 0.01$) at two symmetrically placed locations than at midspan ($\alpha = 0.18$). As the arch rise parameter is increased further, the cross-sectional area of the optimal design shrinks to zero at midspan and two symmetrical locations, where hinges of zero bending moment develop.

Optimal values of the nondimensional fundamental frequency, ω, are plotted versus $\bar{\alpha}$ in Fig. 8 as solid curves. The dashed curves represent second natural frequencies of optimal designs for which the fundamental frequency is single modal. (In fact, we also computed the third natural frequencies in order to check their assumed non-coalescense with the optimal fundamental frequencies.) The fundamental frequencies ω_{cu} and the second natural frequencies for circular arches of constant cross-section correspond to fully constrained design and can be identified at the right hand side of the figure, where $\bar{\alpha} = 1$. These frequencies for uniform circular arches were earlier depicted by the two lower curves in Fig. 2. The frequencies at the left hand side of Fig. 8, where $\bar{\alpha} = 0$, are those that correspond to geometrically unconstrained optimal design.

For the cases $c = 0$ and $c = 1$ in Fig. 8, the optimal designs for $0 < \bar{\alpha} < 1$ are associated with a symmetric fundamental vibration mode, and only the geometrically unconstrained design ($\bar{\alpha} = 0$) is bimodal. For $c = 2$, 3 and 4, we obtain designs with a single symmetric fundamental mode if $\bar{\alpha}$ is greater than the value at which the solid and dashed curves coalesce, and we have bimodal solutions to the left of those points in Fig. 8. To the left of the points marked by an $\times$, the geometric constraint is inactive and the optimal designs and frequencies then do not vary

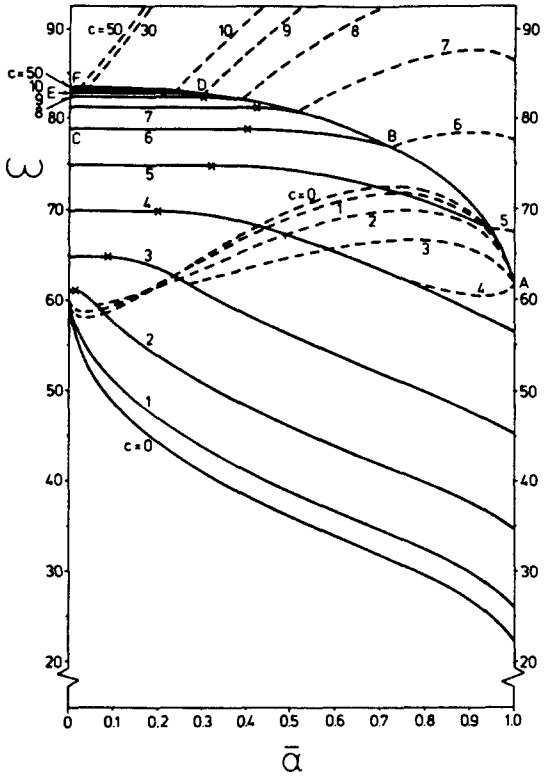

Fig. 8. Natural frequencies ω vs minimum area constraint value $\bar{\alpha}$ for optimal clamped circular arches of different arch rise c. Solid curves indicate optimal fundamental frequencies, and dashed curves denote second natural frequencies. ×-marks indicate transition between $\bar{\alpha}$-dependent and $\bar{\alpha}$-independent bimodal designs.

with $\bar{\alpha}$. For example, as discussed in relation to Fig. 4(c), this threshold between geometric constraint dependent and independent optimal designs is $\bar{\alpha} = 0.084$ when $c = 3$.

For $c = 4$, the optimal designs are seen to be bimodal for a broad range of $\bar{\alpha}$ values. Only for values of $\bar{\alpha}$ close to 1, implying nearly uniform designs, are the solutions single modal (with a symmetric mode). Now, if c is taken to be $c = 4.464$, then the uniform design is bimodal (see the intersection point for the two lower curves in Fig. 2), and when circular arches with $c = 4.464$ are optimized, we find that the optimal designs are bimodal for *all* $\bar{\alpha}$ values ($0 \leq \bar{\alpha} \leq 1$). Increasing c slightly beyond the value of 4.464, the optimal designs are bimodal for a broad range of $\bar{\alpha}$ values, with the exception of values of $\bar{\alpha}$ close to 1, where the optimal single mode designs are now associated with an antisymmetric fundamental vibration mode. As c is increased further, the range of $\bar{\alpha}$ values corresponding to a single fundamental frequency with an antisymmetric mode increases in size.

For $c = 6$, for example, the optimal fundamental frequency ω is defined by the curve *ABC* in Fig. 8. In segment *AB*, it is associated with a single, antisymmetric mode, while it is bimodal in segment *BC*. For $c = 9$, the governing curve is *ABDE*, with an antisymmetric mode in segment *ABD*.

Note that segment *AB* is valid for both $c = 6$ and $c = 9$, so that the optimal designs in this range are the same for both cases. This means, e.g. that the optimal area function associated with $\bar{\alpha} = 0.8$ in Fig. 6(a) (for $c = 9$) is also valid for the case $c = 6$. But this implies further that the $\bar{\alpha} = 0.8$ design in Fig. 6(a) is also optimal for all values of c higher than $c = 6$. Along similar lines, the optimal area function with $\bar{\alpha} = 0.5$ in Fig. 6(b) (for $c = 9$) is valid for $c = 8, 9, \ldots$.

As c is increased, the $\bar{\alpha}$ range for single (antisymmetric) mode solutions increases, and the solid curves for the optimal fundamental frequencies approach the *limiting curve ABDF* (where *F* is only very slightly above the frequency for geometrically unconstrained design with $c = 50$).

The existence of a limiting curve can be explained easily. If the optimal design turns out to be symmetrical and the fundamental eigenvalue ω_1^2 is associated with a single antisymmetric mode $z_1(x)$, the second term on the left hand side of (25) is zero for $i = 1$, and we have $\gamma = 0$. It

then follows that $y_0(x)$, and hence c, are not involved in the equations which govern the optimal cross-sectional area function $\alpha(x)$. Each point on the limiting curve *ABDF* in Fig. 8 is then valid for sufficiently high values of c. In other words, for a given geometric constraint value $\bar{\alpha}$, the fundamental frequency of a clamped circular arch cannot be increased above that on the limiting curve, no matter what value c has.

5. OPTIMIZATION OF FORM AND CROSS-SECTIONAL AREA OF CLAMPED ARCHES

As in the previous section, we consider the case of clamped ends and $p = 3$, but now we use both the arch form $y_0(x)$ and the cross-sectional area $\alpha(x)$ as design variables. The arch length parameter β^2 is specified. However, results are presented in terms of the parameter c defined by (15), in order to facilitate comparisons with the previous results for circular arches.

Optimal fundamental frequencies, ω, for our problem with two design variables are plotted versus $\bar{\alpha}$ in Fig. 9 as solid curves. The dashed curves again represent second natural frequencies for single mode optimal designs, while the dash-dotted curves for $c = 1$, 2 and 3 give optimal frequencies for the circular arch, for comparison purposes, and are repeated from Fig. 8. The curve for $c = 0$ is also the same as in Fig. 8, since the case of the straight beam does not involve the second design variable $y_0(x)$; its second frequency is plotted in Fig. 8 and is not shown in Fig. 9.

For $c = 1$, 2 and 3, the optimal designs are associated with a single symmetric mode if $\bar{\alpha}$ is high enough, and the solution is bimodal otherwise. The optimal forms and cross-sectional area functions are all found to be symmetric. It then follows from (29) that the optimal forms are proportional to the fundamental symmetric mode (as long as the simple or double fundamental eigenfrequency is associated with such a mode) and the optimal forms thus have zero slope at the ends.

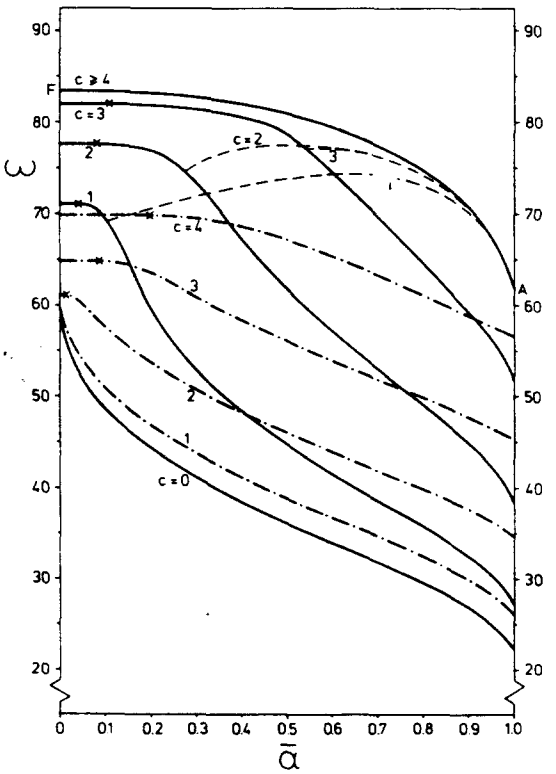

Fig. 9. Natural frequencies ω vs minimum area constraint value $\bar{\alpha}$ for clamped arches optimized both with respect to form $y_0(x)$ and cross-sectional area $\alpha(x)$. Parameter c denotes the rise of a corresponding circular arch having the same length as the optimal arch. Solid curves indicate optimal fundamental frequencies and dashed curves denote second natural frequencies, when both $y_0(x)$ and $\alpha(x)$ are design variables. Dashed–dotted curves represent optimal fundamental frequencies (from Fig. 8) when only $\alpha(x)$ is a design variable. ×-marks indicate transition between $\bar{\alpha}$-dependent and $\bar{\alpha}$-independent bimodal designs.

For $c \geq 4$, the optimal fundamental frequencies lie on curve AF in Fig. 9, which is the same limiting curve as $ABDF$ in Fig. 8. The optimal area functions $\alpha(x)$ are then the same as those corresponding to the limiting curve in Fig. 8. For example, if $c \geq 4$ and $\bar{\alpha}$ is equal to 0.8 or 0.5, the optimal area functions are the same as those shown in Figs. 6(a, b), respectively; also, if c is large enough, e.g. if $c = 6, 7, \ldots$, when $\bar{\alpha} = 0.8$ as in Fig. 6(a), or if $c = 8, 9, \ldots$, when $\bar{\alpha} = 0.5$ as in Fig. 6(b), the circular form is included among the optimal ones. Thus, for $c \geq 4$ the arch forms $y_0(x)$ are not unique. The optimal fundamental frequencies lying on curve AF are then generally single modal with an antisymmetric mode, but for each $\bar{\alpha}$ value there is an arch form (with zero slope at the ends) for which the optimal frequency is bimodal, and then also associated with a symmetric mode.

While the optimal frequencies on curve AF are uniquely determined by the optimal cross-sectional area function $\alpha(x)$ and its associated antisymmetric fundamental vibration mode, which is independent of $y_0(x)$, the second natural frequencies with symmetric modes not only depend on $\alpha(x)$, but also on $y_0(x)$. Since $y_0(x)$ is not unique for $c > 4$, second natural frequencies are not indicated in Fig. 9 for such c values.

Some optimal forms and cross-sectional areas are illustrated in Figs. 10–13, along with the associated fundamental mode(s). In Figs. 10, 11, 12(c), the geometrically unconstrained solutions for $c = 1$, 2 and 3 are shown, respectively. As seen by the existence of the ×-marks in Fig.

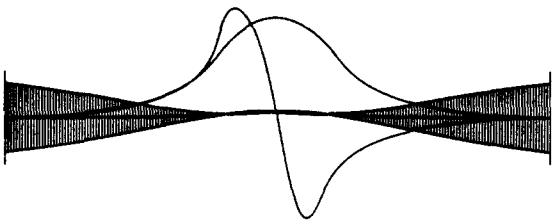

Fig. 10. The optimal design (form and cross-sectional area) of a clamped arch with $c = 1$ (and $p = 3$) for $0 \leq \bar{\alpha} \leq 0.03$ (inactive constraint). The optimal frequency $\omega = 71.1$ is bimodal, and $\omega/\omega_{cu} = 2.73$.

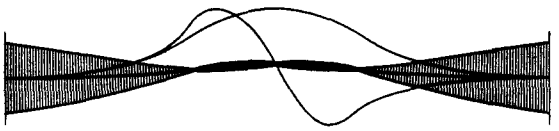

Fig. 11. The optimal design (form and cross-sectional area) of a clamped arch with $c = 2$ (and $p = 3$) for $0 \leq \bar{\alpha} \leq 0.07$ (inactive constraint). The optimal frequency $\omega = 77.6$ is bimodal, and $\omega/\omega_{cu} = 2.24$.

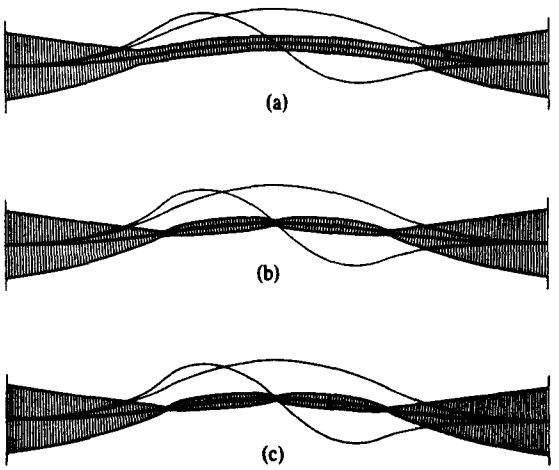

Fig. 12. Optimal designs (forms and cross-sectional areas) of clamped arches with $c = 3$ (and $p = 3$). (a) Design for $\bar{\alpha} = 0.5$ (active constraint), $\omega = 78.7$ (bimodal), $\omega/\omega_{cu} = 1.74$. (b) Design for $\bar{\alpha} = 0.2$ (active constraint), $\omega = 81.9$ (bimodal), $\omega/\omega_{cu} = 1.81$. (c) Optimal design for $0 \leq \bar{\alpha} \leq 0.10$ (inactive constraint), $\omega = 82.0$ (bimodal), $\omega/\omega_{cu} = 1.81$.

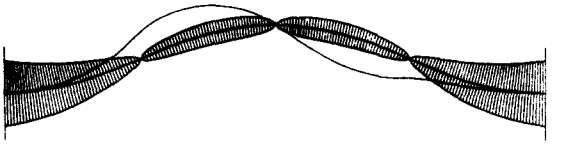

Fig. 13. Optimal design (form and cross-sectional area) of a clamped arch with $c = 9$, $\bar{\alpha} = 0$ (and $p = 3$). The optimal frequency $\omega = 83.5$ is single modal for the arch form shown, and $\omega/\omega_{cu} = 1.35$. The cross-sectional area function is optimal for $\bar{\alpha} = 0$ and any $c \geq 4$, but the optimal arch form is then not unique.

9, there are no cross-sections with zero area in these designs, i.e. the constraint is inactive (and the optimal designs are $\bar{\alpha}$-independent) for sufficiently small values of $\bar{\alpha}$. The cross-sectional area exhibits three local minima.

Geometrically constrained optimal designs are presented for $c = 3$ in Figs. 12(a, b), with $\bar{\alpha} = 0.5$ and 0.2, respectively. It is interesting to compare the cross-sectional area distributions in Fig. 12 with those in Fig. 4, where the arch form is circular but the same combinations of c and $\bar{\alpha}$ are prescribed. For $\bar{\alpha} = 0.5$, the optimal circular arch is associated with a single symmetric mode, whereas the optimal solution in the general case is bimodal. For $\bar{\alpha} = 0.2$ and 0, the optimal circular arches have smallest area in the center of the span and increasing area toward the clamped ends, while the optimal area functions in Figs. 12(b, c) have three local minima.

Finally, Fig. 13 illustrates the optimal cross-sectional area function $\alpha(x)$ at point F in Fig. 9, together with an optimal arch form function $y_0(x)$ for the case $c = 9$. The area function $\alpha(x)$ in Fig. 13 is equal to zero at three inner hinges of zero bending moment (Type I singularities [12]) and is valid for $c \geq 4$. For any specified values of c in this range, there is a class of forms $y_0(x)$ which, together with the optimal area function $\alpha(x)$, will be optimal, i.e. will possess the highest possible fundamental frequency, $\omega = 83.5$.

6. SUMMARY

The optimization of the fundamental frequency of shallow arches depends on the arch length parameter β^2 (or, equivalently, on the parameter c defined by (15)) and on the value of the minimum allowable area $\bar{\alpha}$. Optimal frequencies associated with $\bar{\alpha} = 0$ and $\bar{\alpha} = 1$ are presented in Fig. 14 as a function of c, together with fundamental frequencies for standard (comparison) arches. These results (for clamped arches) can be described in terms of four classifications.

(1) *Arches of circular form and constant cross-section*

Curve *ABK* in Fig. 14 represents the lowest frequency associated with a symmetric vibration mode of a uniform circular arch, while curve *HDBC* represents the lowest frequency for an antisymmetric mode. (These curves are also shown in Fig. 2.) The *fundamental* frequency of the arch type chosen here for comparison purposes is thus given by curve *ABC*, and our objective has been to raise this curve as much as possible, without changing the span, length, volume, and material of the arch.

(2) *Arches of optimal form and constant cross-section*

If only the arch form is used as a design variable, the optimal ω-curve is given by *ADBC*, see Ref. [6]. This corresponds to $\bar{\alpha} = 1$ in Fig. 9. In segment *AD*, the optimal forms are unique and have zero slope at the ends; in segment *DBC*, they are not unique (e.g. the circular form is optimal in segment *BC*).

(3) *Arches of circular form and optimal cross-sectional area distribution*

The results of Section 4, in which the arch form is specified to be circular and only the cross-sectional area function is used as a design variable, lead to curve *EF* in Fig. 14 if no geometric constraint of minimum area is invoked (i.e. $\bar{\alpha} = 0$ in Fig. 8). A bimodal solution exists for all values of c. As c increases, the curve approaches the limiting value $\omega = 83.5$, which corresponds to point F in Fig. 8. The increase in fundamental frequency from that of a uniform circular arch (curve *ABC*) is 167% for $c = 0$ and 35% for large values of c.

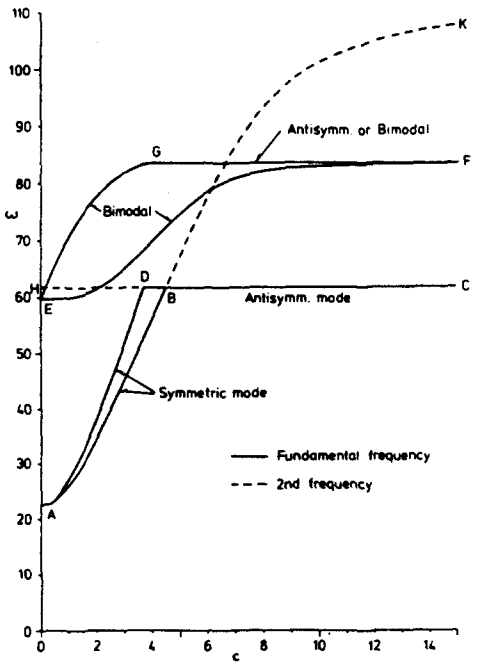

Fig. 14. Fundamental frequencies ω vs parameter c different arches with clamped ends. Curve ABC: ω for arches of circular form and constant cross-section ($\alpha \equiv 1$). Curve $ADBC$: Arches of optimal form and constant cross-section ($\alpha \equiv \bar{\alpha} = 1$). Curve EF: Arches of circular form and optimal, geometrically unconstrained cross-sectional area distribution ($\bar{\alpha} = 0$). Curve EGF: Arches of optimal form and optimal, geometrically unconstrained area distribution ($\bar{\alpha} = 0$). The ordinate for the point A is $\omega = 22.373$, the ordinates for the points H, D, B and C are $\omega = 61.673$, and the ordinates for the points G and F are $\omega = 83.5$. The abscissa for the point D is $c = 3.69$, the abscissa for the point G is $c \simeq 4$, and the abscissa for the point B is $c = 4.464$.

(4) *Arches of optimal form and cross-sectional area distribution*

Curve EGF in Fig. 14 represents the geometrically unconstrained results from Section 5 (see $\bar{\alpha} = 0$ in Fig. 9), in which the arch form $y_0(x)$ and area $\alpha(x)$ are both treated as design variables. In comparison with the circular arches with optimal area distribution (curve EF), the improvement in the fundamental frequency is only significant for small values of c. However, relative to the uniform circular arch, the fundamental frequency is increased by 173% for $c = 1$, 124% for $c = 2$, 81% for $c = 3$, and 35% for $c \geq 4.464$.

In addition to the above summary of the optimal eigenvalues, we should also comment on the general characteristics of the optimal area distributions. For small values of c, the arch has smallest area in its central portion and then increasing area toward the ends (e.g. see Figs. 4, 10 and 11). As c increases, the designs form bulges on both sides of the center (e.g. see Figs. 5, 6 and 12). The locations and extent of these bulges depend on $\bar{\alpha}$ (e.g. see Fig. 6). For sufficiently high values of c, the area of geometrically unconstrained optimal designs becomes equal to zero at three points of the span (the center and two symmetrically placed locations), where hinges develop.

It is noteworthy that the geometrically unconstrained, optimal arches in Sections 4 and 5 do not have points of zero area for a range of c values. However, if only a single modal formulation had been used, such points would be present in *all* the geometrically unconstrained designs, and most of these designs would be non-optimal. In fact, only in cases of bimodality for which the coalescence of eigenvalues takes place in the very limit of geometrically unconstrained design (i.e. as $\bar{\alpha} \to 0$) is a single mode formulation sufficient. Some cases of this type can be found in Ref. [13].

Finally, two features of the results of this investigation should be reiterated. First of all, when the optimal form is unique, it has zero slope at clamped ends and is therefore convex in regions adjacent to such ends. Secondly, the optimal solutions are generally bimodal (i.e. the fundamental frequency is a double eigenvalue). Bimodal solutions were found previously for

buckling optimization of a clamped column[7]. The present investigation shows that a bimodal formulation may also be required when optimizing a continuous structure with respect to vibrations.

Acknowledgements—The second author was supported by the U.S. National Science Foundation under grant CME-7920781, a NATO Senior Fellowship, and grant no. 16-3077 from the Danish Council for Scientific and Industrial Research (which also covered computational costs).

REFERENCES

1. N. Olhoff, Optimal design with respect to structural eigenvalues. In *Theoretical and Applied Mechanics, Proc. XVth Int. Cong. Th. Appl. Mech.*, Toronto, 1980 (Edited by F. P. J. Rimrott and B. Tabarrok), pp. 133–149. North-Holland, Amsterdam (1980).
2. K. Thermann, Zum optimalen Entwurf eines schwingenden Kreisbogenträgers. *Z. Angew. Math. Mech.* **52**, T156–T158 (1972).
3. A. B. Smirnov and V. A. Troitskii, Optimization of natural vibration frequencies of curvilinear thin elastic rods (*in* Russian). *MTT* (*Mechanics of Solids*) **14**, 162–168 (1979).
4. J. Blachut and A. Gajewski, On unimodal and bimodal optimal design of funicular arches. *Int. J. Solids Structures* **17**, 653–667 (1981).
5. J. Blachut and A. Gajewski, Unimodal and bimodal optimal designs of extensible arches with respect to buckling and vibrations. To appear in *Opt. Control Appls. Meths.*
6. R. H. Plaut and N. Olhoff, Optimal forms of shallow arches with respect to vibration and stability. *J. Struct. Mech.* to be published.
7. N. Olhoff and S. H. Rasmussen, On single and bimodal optimum buckling loads of clamped columns. *Int. J. Solids Structures* **13**, 605–614 (1977).
8. B. L. Karihaloo and F. I. Niordson, Optimum design of vibrating cantilevers. *J. Optimiz. Th. Appl.* **11**, 638–654 (1973).
9. G. J. Simitses and I. H. Rapp, III, Snapping of low arches with nonuniform stiffness. *J. Engng Mech. Div. ASCE* **103**, 51–65 (1977).
10. E. J. Haug and B. Rousselet, Design sensitivity analysis in structural mechanics. II. Eigenvalue variations. *J. Struct. Mech.* **8**, 161–186 (1980).
11. E. F. Masur, Optimal structural design under multiple eigenvalue constraints. To appear in *Int. J. Solids Structures*.
12. N. Olhoff, Optimization of vibrating beams with respect to higher order natural frequencies. *J. Struct. Mech.* **4**, 87–122 (1976).
13. N. Olhoff, Maximizing higher order eigenfrequencies of beams with constraints on the design geometry. *J. Struct. Mech.* **5**, 107–134 (1977).

APPENDIX

Here we outline the procedure developed for solution of the equations governing the bimodal optimization problem with $y_0(x)$ and $\alpha(x)$ as design variables. The solution procedure for the problem where only $\alpha(x)$ is a design variable is contained as a special case. The procedure is numerical and consists of successive iterations based on a finite difference formulation of equations obtained by a formal integration of the problem. We first give an account of the formal integration and then present the iteration scheme.

Integrating the vibrating arch equation (25) twice, we get

$$\alpha^p z_i'' + 4y_0\left[\int_0^1 \alpha^{-1}\,dx\right]^{-1}\int_0^1 z_i y_0''\,dx + a_i + b_i x = f_i(x), \quad i = 1,2, \tag{A1}$$

where a_i and b_i, $i = 1,2$, are integration constants to be determined by the boundary conditions and $f_i(x)$, $i = 1,2$, is taken to be

$$f_i(x) = \omega_i^2\left[\int_0^x\int_0^\xi \alpha z_i\,d\eta\,d\xi - x\int_0^1\int_0^\xi \alpha z_i\,d\eta\,d\xi\right], \quad i = 1,2, \tag{A2}$$

so that $f_i(0) = f_i(1) = 0$. If both arch ends are simply supported, we will then have $a_i = b_i = 0$, $i = 1,2$, but if other boundary conditions are specified, a_i and b_i will generally be different from zero.

Assuming $\alpha(x)$, $y_0(x)$, and $f_i(x)$, $i = 1,2$, to be known, the second order differential equation (A1) can now be discretized along with the given set of boundary conditions such that we obtain a system of linear, algebraic equations for the discrete values of $z_i(x)$ and the constants a_i and b_i. Solving this system of equations, we obtain $z_i(x)$, $i = 1,2$, and thereby also $z_i''(x)$ and $m_i(x)$.

It should be noted that the coefficient matrix for the set of algebraic equations for the discrete values of $z_i(x)$ and the constants a_i and b_i is generally fully packed, since $z_i(x)$ appears under an integral sign in the second term on the r.h.s. of (A1). This can be avoided by moving this term to the r.h.s. of (A1) so as to include it in the $f_i(x)$ expression, or, for one of the cases ($i = 1$ or $i = 2$), by making possible symmetry assumptions. However, for the examples presented in Sections 4 and 5, we did not want to lose possible non-symmetric optimal designs, and it turned out that rearranging (A1) as described generally led to unacceptable inaccuracies in extensible modes, irrespective of whether the integration leading to (A2) was performed in alternative ways.

The arch form $y_0(x)$ is obtained by integrating the optimality condition (27) twice, i.e.

$$y_0(x) = a + bx - \beta^2\frac{(1-\gamma)z_1(x)\int_0^1 z_1 y_0''\,dx + \gamma z_2(x)\int_0^1 z_2 y_0''\,dx}{(1-\gamma)\left[\int_0^1 z_1 y_0''\,dx\right]^2 + \gamma\left[\int_0^1 z_2 y_0''\,dx\right]^2}, \tag{A3}$$

where the integration constants a and b are determined by the boundary conditions $y_0(0) = y_0(1) = 0$. If the arch ends are clamped or simply supported, we have $a = b = 0$. If at a certain stage of the iterative solution procedure we found that $\gamma = 0$ and $\int_0^1 z_1 y_0'' \, dx = 0$, or $\gamma = 1$ and $\int_0^1 z_2 y_0'' \, dx = 0$, implying that (A3) is no longer valid, i.e. that $y_0(x)$ is non-unique, we checked whether $\alpha(x)$ was symmetrical (which always turned out to be the case in our examples), and then applied (29) (with $z_1(x)$ denoting the symmetric mode) in order to determine uniquely one of the members of the class of optimal $y_0(x)$ functions.

For the general arch optimization problem associated with given values of $\bar{\alpha}$ and β^2 (and $p = 3$ in our examples), we have constructed the following scheme of successive iterations:

START: Assume $y_0(x)$, $\alpha(x)$, $z_i(x)$, γ, ν and ω_i.

I Compute $f_i(x)$ from (A2).

II Determine $z_i(x)$ from (A1), orthonormalize these functions according to (16) and (17), and compute $z_i''(x)$.

III Compute $y_0(x)$ and $y_0''(x)$ from (A3) and (27). (If (A3) and (27) are invalid, determine $y_0(x)$ from (29) if $\alpha(x)$ is symmetric, and compute $y_0''(x)$.) Normalize $y_0(x)$ and $y_0''(x)$ such that (11) is satisfied.
Go to I if $y_0(x)$ and hence $z_i(x)$ have not converged within the inner loop I–III.

IV Compute $m_i(x)$ from (32).

V Compute A and B from (34a, b).

VI Compute C from (34c). Compute $\alpha(x)$ (and thereby $\alpha_u(x)$, x_u, and x_c) from (35) and (36c). If (37) is not satisfied for the applied value of ν, determine a new value of ν as part of a Newton–Raphson procedure to meet (37), and repeat VI.

VII Compute A, B and C from (34), $\alpha_u(x)$ from (36c), and ω_i from (38), for different values of γ, $0 \le \gamma \le 1$. If $\omega_1 < \omega_2$ or $\omega_2 < \omega_1$ for all $\gamma \in 0 \le \gamma \le 1$, go to X.

VIII Compute A, B and C from (34), and $\alpha_u(x)$ from (36c). If (40) is not satisfied for the applied value of γ, determine a new value of γ as part of a bisection procedure to meet (40), and repeat VIII.

IX Compute $\omega_1 (= \omega_2)$ from (38) for the solution γ, $0 < \gamma < 1$, obtained in VIII. Set $\omega = \omega_i$.
Go to V, if γ, and hence ν, $\alpha(x)$, x_u and x_c, have not converged within the inner loop V–IX. Else go to XI.

X If $\omega_1 < \omega_2$ for all $\gamma \in 0 \le \gamma \le 1$, set $\omega = \omega_1$ and $\gamma = 0$. If $\omega_2 < \omega_1$ for all $\gamma \in 0 \le \gamma \le 1$, set $\omega = \omega_2$ and $\gamma = 1$.

XI Go to I if ω, and hence all other iterates, have not converged within the main loop I–XI.

END

If $y_0(x)$ is not treated as a design variable, but is specified, step III and the subsequent "go to" statement are bypassed.

In order to obtain the locations of the constrained intervals accurately, and for precise modeling of functional behavior, the number of stations in the interval $0 \le x \le 1$ was taken to be large, and the computations were performed in double precision. The numerical stability of the solutions obtained was checked through computations based on different numbers of equally spaced stations.